Journal of
Mechanical
Science and
Technology

Journal of Mechanical Science and Technology 21 (2007) 699~707

Inelastic Constitutive Models for the Simulation of a Cyclic Softening Behavior of Modified 9Cr-1Mo Steel at Elevated Temperatures

Gyeong-Hoi Koo[a,*], Jae-Han Lee[a]

[a]*Korea Atomic Energy Research Institute*

(Manuscript Received October 23, 2006; Revised March 23, 2007; Accepted March 23, 2007)

Abstract

In this paper, the inelastic constitutive models for the simulations of the cyclic softening behavior of the modified 9Cr-1Mo steel, which has a significant cyclic softening characteristic especially in elevated temperature regions, are investigated in detail. To do this, the plastic modulus, which primarily governs the calculation scheme of the plasticity, is formulated for the inelastic constitutive models such as the Armstrong-Frederick model, Chaboche model, and Ohno-Wang model. By implementing the extracted plastic modulus and the consistency conditions into the computer program, the inelastic constitutive parameters are identified to present the best fit of the uniaxial cyclic test data by strain-controlled simulations. From the computer simulations by using the obtained constitutive parameters, it is found that the Armstrong-Frederick model is simple to use but it causes significant overestimated strain results when compared with the Chaboche and the Ohno-Wang models. And from the ratcheting simulation results, it is found that the cyclic softening behavior of the modified 9Cr-1Mo steel can invoke a ratcheting instability when the applied cyclic loads exceed a certain level of the ratchet loading condition.

Keywords: Modified 9Cr-1Mo steel; Inelastic constitutive model; Ratcheting; Armstrong-Frederick model; Chaboche model; Ohno-wang model; Plastic modulus; Cyclic instability; Cyclic softening

1. Introduction

Recently, the KALIMER (Korea Advanced Liquid Metal Reactor) (Han, 2004) has been selected as a candidate reactor concept of the GEN-IV (Generation IV) reactors. While the current Generation II and III nuclear power plant designs provide an economically and publicly acceptable electricity supply in many countries, the GEN-IV nuclear energy system is now under development by the leadership of GIF (Generation IV International Forum) to meet the further needs for a safety, sustainability, economics, and nuclear non-proliferation.

Among the GEN-IV goals, economics is one of the important factors to substantiate a GEN-IV nuclear energy system in the future. To accomplish its goal of an economics, the usage of advanced materials such as FMS (Ferritic/Martensitic Steel) and ODS (Oxide Dispersion-Strengthened) steel is one promising way to enhance the economics of the GEN-IV nuclear energy system (Nibe, 2001). This is an important issue especially in the field of high temperature reactor designs (Ruggles, 1994). A modified 9Cr-1Mo steel, which is a well-known FMS material and now under consideration to be applied to the structural design of the KALIMER-600, has many advantages such as high yield strength, good thermal conductivity, small thermal expansion, and excellent resistance to stress corrosion cracking.

To use the modified 9Cr-1Mo steel for the GEN-IV reactor design, it is necessary to develop an inelastic

*Corresponding author. Tel.: +82 42 868 2950
E-mail address: ghkoo@kaeri.re.kr

structural analysis methodology relevant to the material. Recently the researches on modified 9Cr-1Mo steel have been done to investigate the ratcheting of viscoplastic material with cyclic softening (Yaguchi, 2005) by the experiments and the constitutive equation of the Ohno-Wang model. In this paper, various inelastic constitutive models which can predict the cyclic ratcheting behavior of a modified 9Cr-1Mo steel are investigated and compared in detail to find out the most appropriate model for the GEN-IV reactor design. To do this, the constitutive parameters corresponding to the Armstrong and Frederic Model (Armstrong, 1966; Bari, 2000), the Chaboche Model (Chaboche, 1983, 1989), and the Ohno and Wang Model (Ohno and Wang, 1993) are identified by using the test data and verified by a comparison between the test data and strain-controlled simulations. Actually the cyclic ratcheting simulations by the inelastic constitutive models are primarily governed by the plastic modulus, which can be obtained by a coupling of the kinematic hardening rule through a consistency condition. In this paper, the plastic modulus corresponding to each constitutive model are formulated and implemented into a PARA-ID computer program with the radial return algorithm (Simo, 1985). With the ratcheting load conditions of the constant stress amplitude and the mean stress, the cyclic ratcheting behaviors of the modified 9Cr-1Mo steel are investigated by using stress-controlled simulations. The simulation results obtained by each constitutive model are compared and discussed. The possibility of the progressive ratcheting instability phenomena due to the significant cyclic softening characteristics of the modified 9Cr-1Mo steel are investigated by using the Chaboche model.

2. Inelastic constitutive models

2.1 Kinematic hardening models

2.1.1 Armstrong-Frederick model

To simulate the plastic behavior of materials, the simplest model has been proposed by Prager (1956) with the following kinematic hardening model of the deviatoric backstress evolution;

$$\dot{\alpha}_{ij} = C\dot{\varepsilon}^{p}_{ij} \tag{1}$$

In this model, the yield surface moves linearly with the plastic strain and the hysteresis loop is bilinear. Therefore, this model can not represent the nonlinear part of the hysteresis loop. Furthermore, this model only produces a closed hysteresis loop for a prescribed uniaxial stress cycle with a mean stress, thus it can not simulate a ratcheting behavior.

To overcome the deficiency of the Pager model, Armstrong and Frederick have proposed a nonlinear kinematic hardening model, which can describe the nonlinear parts of the hysteresis loop with a memory effect of the strain path, as follows;

$$\dot{\alpha}_{ij} = \frac{2}{3}C\dot{\varepsilon}^{p}_{ij} - \gamma\alpha_{ij}\dot{p} \tag{2}$$

In the above equation, $\dot{p}$ is the evolution of the accumulated plastic strain expressed as

$$\dot{p} = \left|\dot{\varepsilon}^{p}_{ij}\right| = \left[\frac{2}{3}\dot{\varepsilon}^{p}_{ij}\dot{\varepsilon}^{p}_{ij}\right]^{1/2} \tag{3}$$

The symbols used in the equations are expressed in the Nomenclature. As shown in Eq. (2), it is difficult to fully describe the nonlinear part of the hysteresis loop with only a single backstress function.

2.1.2 Chaboche model

To improve the deficiency of the Armstrong and Frederick model, Chaboche has proposed a 'decomposed' nonlinear kinematic hardening model as follows;

$$\dot{\alpha}_{ij} = \sum_{k=1}^{n}(\dot{\alpha}_{ij})_k = \sum_{k=1}^{n}\left(\frac{2}{3}C_k\dot{\varepsilon}^{p}_{ij} - \gamma_k(\alpha_{ij})_k\dot{p}\right) \tag{4}$$

As expressed in Eq. (4), the Chaboche kinematic hardening model is basically a superposition of several Armstrong-Frederick hardening model. Initially, Chaboche proposed a model with 3-decomposed rules (n = 3), which has three segments of a stable hysteresis loop. This model suggests that the first rule (α_1) should have a very large modulus at the beginning of the hardening behavior and it should stabilize very quickly. The second rule (α_2) should have a function for simulating the transient nonlinear part. Finally, the third rule (α_3) should have a function for the linear hardening behavior of the hysteresis loop throughout all the strain ranges.

2.1.3 Ohno and Wang model

Ohno and Wang have proposed the multi-decom-

posed nonlinear kinematic hardening rules (Ohno, 1993) based on dividing the hardening curve into many linear segments like the multilinear hardening model. They introduced a slight nonlinearity for each decomposed rule at the transition from a linear kinematic hardening to a stabilized critical state as follows;

$$\dot{\alpha}_{ij} = \sum_{k=1}^{n}(\dot{\alpha}_{ij})_k = \sum_{k=1}^{n}\left\{\frac{2}{3}C_k\dot{\varepsilon}_{ij}^{p} - \gamma_k(\alpha_{ij})_k\left\langle\dot{\varepsilon}_{ij}^{p}\bullet\frac{(\alpha_{ij})_k}{f(a_k)}\right\rangle\left(\frac{f(a_k)}{C_i/\gamma_i}\right)^{m_i}\right\} \tag{5}$$

In the above equation a slight nonlinearity is expressed with a multiplier with a power of m_i and it has a role of preventing the stress-controlled hysteresis loop from being a closed loop and causing a ratcheting behavior.

2.2 Cyclic softening model

For the isotropic hardening rule, Chaboche (1991) has proposed the constitutive model as follows;

$$\dot{R} = b[Q - R]\ \dot{p} \tag{6}$$

where b and Q are material parameters and R is the drag stress. When the initial value $R = 0$, integrating Eq. (6) gives:

$$R = Q\ (1 - e^{-bp}) \tag{7}$$

As expressed in Eq. (7), the drag stress R drastically increases to a certain extent of the initial cycles with an increasing accumulated plastic strain and it is steadily saturated to a certain level. Actually, the modified 9Cr-1Mo steel has a salient feature of the cyclically softening characteristics especially in the high temperature region. To describe the cyclic softening behavior exponentially decreased drag stress function with increments of the plastic strain, the material parameter Q has a negative value. In the above equation, the material parameter Q can be represented as

$$Q = Q_M + (Q_0 - Q_M)\ e^{-2\mu q} \tag{8}$$

where Q_M, Q_0, and μ are material parameters to be determined and $q = \left\|\dot{\varepsilon}_{ij}^{p}/2\right\|$.

2.3 Formulations of the plastic modulus

The total strain increment tensor is the sum of the elastic and plastic strain increment tensors as follows;

$$\dot{\varepsilon}_{ij} = \dot{\varepsilon}_{ij}^{e} + \dot{\varepsilon}_{ij}^{p} \tag{9}$$

From the equation, the elastic strain can be obtained easily by differentiating the elastic potential function with respect to the stress tensor σ_{ij}. Similarly, the plastic flow equations can be obtained with the plastic potential function $g(\sigma_{ij})$, which is a scalar function of the stresses as follows;

$$\dot{\varepsilon}_{ij}^{p} = \lambda\ \frac{\partial g}{\partial\sigma_{ij}} \tag{10}$$

where λ is a positive scale factor of a proportionality, which is zero in the elastic domain, and it is actually derived as

$$\lambda = \frac{1}{H}\left\langle\frac{\partial f}{\partial\sigma_{ij}}\bullet\dot{\sigma}_{ij}\right\rangle \tag{11}$$

where H is the plastic modulus, $< >$ indicates the MacCauley bracket, and the symbol $\bullet$ presents the inner product as $a \bullet b = a_{ij}b_{ij}$. As shown in Eq. (11), the plastic flow vector $\dot{\varepsilon}_{ij}^{p}$ is directed along the normal direction to the surface of the plastic potential. For most stable materials, the flow rule is associative. This means that the plastic potential function and the yield function coincide as $g = f$. In this case, the plastic flow rule is represented as

$$\dot{\varepsilon}_{ij}^{p} = \lambda\ \frac{\partial f}{\partial\sigma_{ij}} \tag{12}$$

and it develops along the normal direction to the yield surface.

Actually, it is well-known that the constitutive equations for the mechanical behavior of materials are generally based on thermodynamical concepts (Chaboche, 1983). In this study, a typical von Mises yield criteria, which is based on the thermodynamic forces associated with two internal state variables such as the kinematic (back stress, α_{ij}) and the isotropic hardening (drag stress, R) variables, is used as follows;

$$f(\sigma_{ij}-a_{ij})=\sqrt{\frac{3}{2}(\tau_{ij}-\alpha_{ij})(\tau_{ij}-\alpha_{ij})}-\sigma_{yo}-R \\ =0 \tag{13}$$

where σ_{ij} is the Cauchy stress tensor, a_{ij} is the total backstress tensor, τ_{ij} is the deviatoric stress tensor of the stress tensor σ_{ij} , α_{ij} is the deviatoric backstress tensor (the current center of the yield surface), σ_{yo} is the initial yield stress, and R is the isotropic hardening variable.

As shown in the equation of the plastic strain evolution from the flow rule of Eq. (12), the simulation for a cyclic behavior primarily depends on the plastic modulus calculation scheme. Most of the nonlinear kinemtaic hardening models are called a coupled model because the plastic modulus calculation is coupled with the kinematic hardening rule through a consistency condition. After applying the consistency condition to the yield criterion of Eq. (13), the evolution of the yield function can be obtained as

$$\dot{f} \equiv \frac{\partial f}{\partial \tau_{ij}}\dot{\tau}_{ij} + \frac{\partial f}{\partial \alpha_{ij}}\dot{\alpha}_{ij} + \frac{\partial f}{\partial R}\dot{R} = 0 \tag{14}$$

Each derivative term can be obtained after differentiating the yield function with respect to the deviatoric stress as follows;

$$\frac{\partial f}{\partial \tau_{ij}}=\frac{3(\tau_{ij}-\alpha_{ij})}{2\sqrt{\frac{3}{2}(\tau_{ij}-\alpha_{ij})(\tau_{ij}-\alpha_{ij})}} \tag{15}$$

$$\frac{\partial f}{\partial \alpha_{ij}} = -\frac{\partial f}{\partial \tau_{ij}} \tag{16}$$

$$\frac{\partial f}{\partial R} = -1 \tag{17}$$

After substituting Eq. (15)–Eq. (17) into Eq. (14), one can obtain

$$\frac{\partial f}{\partial \tau_{ij}}(\dot{\tau}_{ij}-\dot{\alpha}_{ij})-\dot{R}=0 \tag{18}$$

The elasticity relationship between the Cauchy stress and the strain tensor is defined as

$$\dot{\sigma}_{ij}=E_{ijkl}\dot{\varepsilon}^{e}_{kl}=E_{ijkl}(\dot{\varepsilon}_{kl}-\dot{\varepsilon}^{p}_{kl}) \tag{19}$$

where E_{ijkl} is the fourth-order elastic modulus tensor.

For the Armstrong and Frederick model, substituting Eq. (2) and Eq. (19) into Eq. (18) one can obtain the equation as

$$\frac{\partial f}{\partial \sigma_{ij}}\left[E_{ijkl}(\dot{\varepsilon}_{kl}-\dot{\varepsilon}^{p}_{kl})-\left(\frac{2}{3}C\dot{\varepsilon}^{p}_{ij}-\gamma\alpha_{ij}\dot{p}\right)\right] \\ +b(Q-R)\dot{p}=0 \tag{20}$$

where

$$\dot{p} = \left|\dot{\varepsilon}^{p}_{ij}\right| = \left[\frac{2}{3}\dot{\varepsilon}^{p}_{ij}\dot{\varepsilon}^{p}_{ij}\right]^{1/2} = \lambda\left[\frac{2}{3}\frac{\partial f}{\partial \sigma_{ij}}\frac{\partial f}{\partial \sigma_{ij}}\right]^{1/2} \tag{21}$$

After substituting Eq. (12) and Eq.(21) into Eq. (20), one can obtain

$$\frac{\partial f}{\partial \sigma_{ij}}\left[E_{ijkl}\dot{\varepsilon}_{kl} - E_{ijkl}\lambda\frac{\partial f}{\partial \sigma_{kl}} - \frac{2}{3}C\lambda\frac{\partial f}{\partial \sigma_{ij}} + \gamma\alpha_{ij}\lambda\sqrt{\frac{2}{3}\frac{\partial f}{\partial \sigma_{ij}}\frac{\partial f}{\partial \sigma_{ij}}}\right] \\ + b(Q-R)\lambda\sqrt{\frac{2}{3}\frac{\partial f}{\partial \sigma_{mn}}\frac{\partial f}{\partial \sigma_{mn}}} = 0 \tag{22}$$

After some arrangement in terms of $\dot{\varepsilon}_{ij}$ and λ, the following equation can be obtained.

$$\lambda\left(E_{ijkl}\frac{\partial f}{\partial \sigma_{ij}}\frac{\partial f}{\partial \sigma_{kl}} + \frac{2}{3}C\frac{\partial f}{\partial \sigma_{ij}}\frac{\partial f}{\partial \sigma_{ij}} - \gamma\frac{\partial f}{\partial \sigma_{ij}}\alpha_{ij}\sqrt{\frac{2}{3}\frac{\partial f}{\partial \sigma_{ij}}\frac{\partial f}{\partial \sigma_{ij}}} + b(Q-R)\sqrt{\frac{2}{3}\frac{\partial f}{\partial \sigma_{mn}}\frac{\partial f}{\partial \sigma_{mn}}}\right) = \dot{\varepsilon}_{kl}E_{ijkl}\frac{\partial f}{\partial \sigma_{ij}} \tag{23}$$

From Eq. (23) the positive scale factor can be expressed as

$$\lambda = \frac{1}{H}\frac{\partial f}{\partial \sigma_{ij}}E_{ijkl}\dot{\varepsilon}_{kl} \tag{24}$$

where H is defined as a plastic modulus,

$$H = E_{ijkl}\frac{\partial f}{\partial \sigma_{ij}}\frac{\partial f}{\partial \sigma_{kl}} + \frac{2}{3}C\frac{\partial f}{\partial \sigma_{ij}}\frac{\partial f}{\partial \sigma_{ij}} - \gamma\frac{\partial f}{\partial \sigma_{ij}}\alpha_{ij}\sqrt{\frac{2}{3}\frac{\partial f}{\partial \sigma_{ij}}\frac{\partial f}{\partial \sigma_{ij}}} + b(Q-R)\sqrt{\frac{2}{3}\frac{\partial f}{\partial \sigma_{mn}}\frac{\partial f}{\partial \sigma_{mn}}} \tag{25}$$

Substituting Eq. (12) and (24) into Eq. (19) one can obtain the equation as

$$\dot{\sigma}_{ij} = E_{ijkl}\left(\dot{\varepsilon}_{kl} - \lambda\frac{\partial f}{\partial \sigma_{kl}}\right) = \left(E_{ijkl} - \frac{1}{H}E_{ijkl}\frac{\partial f}{\partial \sigma_{ij}}E_{ijkl}\frac{\partial f}{\partial \sigma_{kl}}\right)\dot{\varepsilon}_{kl} \tag{26}$$

Eq.(26) can be rewritten as

$$\dot{\sigma}_{ij} = D_{ijkl}\dot{\varepsilon}_{kl} \tag{27}$$

where the elasto-plastic modulus tensor is defined as

$$D_{ijkl} = E_{ijkl} - \frac{1}{H}E_{ijkl}\frac{\partial f}{\partial \sigma_{ij}}E_{ijkl}\frac{\partial f}{\partial \sigma_{kl}} \tag{28}$$

With the same formulations as the above Armstrong and Frederick Model, the plastic modulus, H for the Chaboche model and the Ohno and Wang model can be expressed respectively as follows;

$$H = E_{ijkl}\frac{\partial f}{\partial \sigma_{ij}}\frac{\partial f}{\partial \sigma_{kl}} + \frac{2}{3}\sum_{k=1}^{n}(C_k)\frac{\partial f}{\partial \sigma_{ij}}\frac{\partial f}{\partial \sigma_{ij}} - \sum_{k=1}^{n}\left[\gamma_k(\alpha_{ij})_k\right]\frac{\partial f}{\partial \sigma_{ij}}\sqrt{\frac{2}{3}\frac{\partial f}{\partial \sigma_{ij}}\frac{\partial f}{\partial \sigma_{ij}}} + b(Q-R)\sqrt{\frac{2}{3}\frac{\partial f}{\partial \sigma_{mn}}\frac{\partial f}{\partial \sigma_{mn}}} \tag{29}$$

$$H = E_{ijkl}\frac{\partial f}{\partial \sigma_{ij}}\frac{\partial f}{\partial \sigma_{kl}} + \frac{2}{3}\sum_{k=1}^{n}(C_k)\frac{\partial f}{\partial \sigma_{ij}}\frac{\partial f}{\partial \sigma_{ij}} - \sum_{k=1}^{n}\left[\gamma_k(\alpha_{ij})_k\left\langle\frac{\partial f}{\partial \sigma_{ij}}\bullet\frac{(\alpha_{ij})_k}{f(a_k)}\right\rangle\left(\frac{f(a_k)}{C_k/\gamma_k}\right)^{m_i}\right]\frac{\partial f}{\partial \sigma_{ij}} + b(Q-R)\sqrt{\frac{2}{3}\frac{\partial f}{\partial \sigma_{mn}}\frac{\partial f}{\partial \sigma_{mn}}} \tag{30}$$

To carry out the simulations, the above equations are implemented into a computer program with a radial return algorithm (Simo, 1985) to compute the cyclic backstress components.

3. Simulation of a cyclic behavior of modified 9Cr-1Mo steel

3.1 Constitutive parameter identifications

In identifying the kinematic hardening parameters, the uniaxial test data of a stable hysteresis loop is required. Figure 1 shows the stable hysteresis loops for various isothermal conditions obtained by the strain-controlled uniaxial specimen tests with the strain rate of 2×10^{-3}/s.

Table 1 shows the kinematic hardening inelastic constitutive parameters for each model determined in this paper for the isothermal condition of 600°C. The parameters for the Prager model and the Armstrong-Frederick model are determined by trials to give the

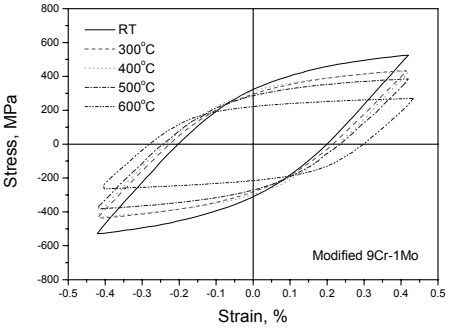

Fig. 1. Hysteresis loops of the Mod.9Cr-1Mo steel by tests.

Table 1. Identified constitutive parameters for the modified 9Cr-1Mo steel at 600 °C.

ID No.	Prager Model		Armstrong-Frederick Model		Chaboche Model		Ohno-Wang Model	
	C (MPa)	γ	C (MPa)	γ	C_{1-9} (MPa)	γ_{1-3}	C_{1-12} (MPa)	γ_{1-12}
1	50,000	-	90,000	1,000	130,000	100,000	103,347	39,604
2	-	-	-	-	183,150	2,500	124,517	9,975
3	-	-	-	-	8,600	1	109,899	4,136
4	-	-	-	-	-	-	28,507	2,460
5	-	-	-	-	-	-	18,335	1,734
6	-	-	-	-	-	-	10,750	1,330
7	-	-	-	-	-	-	8,697	901
8	-	-	-	-	-	-	3,573	677
9	-	-	-	-	-	-	1,950	539
10	-	-	-	-	-	-	1,507	448
11	-	-	-	-	-	-	1,977	383
12	-	-	-	-	-	-	104	336

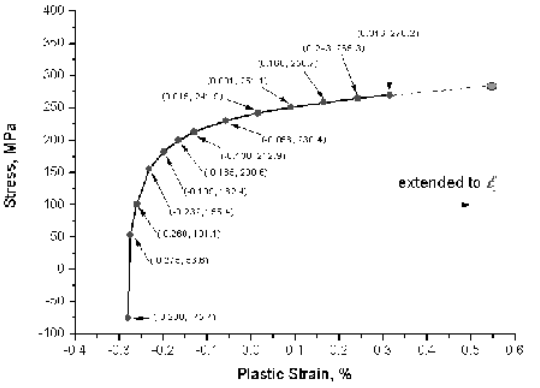

Fig. 2. Stress-plastic strain test data points for a parameter identification of the ohno-wang model.

best fit of the uniaxially tested strain-controlled hysteresis loop data at a stabilized cycle. For the Chaboche model and the Ohno-Wang model, the simple method of the parameter identification proposed by Bari (Bari, 2000) is used. Figure 2 shows the uniaxial test data of the stress-plastic strain curve used to identify the parameters of the Ohno-Wang model.

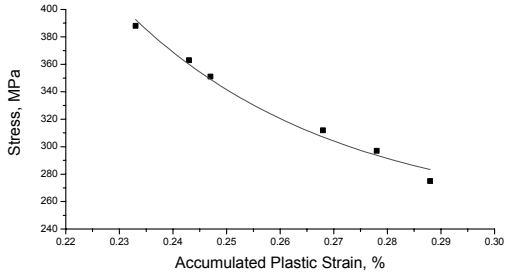

Fig. 3. Cyclic softening behavior of the mod.9Cr-1Mo steel by tests.

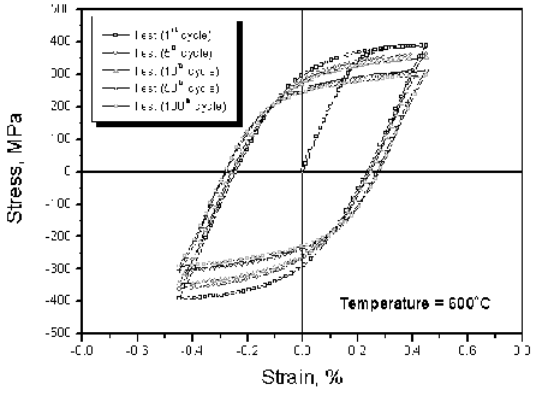

(a) By tests

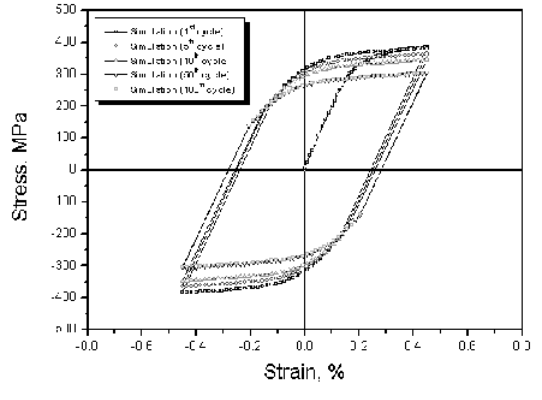

(b) By simulation

Fig. 4. Verification of the cyclic softening simulations by the Chaboche model.

For the cyclic softening parameter identification, the test data of the peak stresses versus the accumulated plastic strains are obtained as shown in Fig. 3 from the cyclic test data. From the curve fitting of the test data, the cyclic softening parameter, b is determined to be 10.4 and the parameter, Q is determined as -87 MPa by the trials of the strain-controlled cyclic simulations to find the best fit of the peak stresses at the end of the 1^{st}, 5^{th}, 10^{th}, 50^{th}, and 100^{th} cycles. Figure 4 shows the comparison of the strain-controlled cyclic behavior between the tests and the simulations by the Chaboche Model. As shown in the figure, the simulation results are in a good agreement with those of the tests for all the cycles presenting a cyclic softening behavior. Therefore, the constitutive parameters determined in this paper are assured to be used for the simulations for the modified 9Cr-1Mo steel.

3.2 Strain-controlled cyclic behavior

Figure 5 shows a comparison of the nonlinear portion of the strain-controlled hysteresis loops obtained by each model. As shown in the figure, the Prager model presents the bilinear characteristics and it can not describe the nonlinear portion at all in the hysteresis loop. Compared with the test results, the Armstrong and Frederick model reveals a nonlinear behavior but has a considerable discrepancy in the nonlinear portion. This means that it is difficult to accurately describe the nonlinear portion of the hystersis loop with the Armstrong-Frederick model. On the other hand, the Chaboche model and the Ohno-Wang model, which have a superposition of several decomposed nonlinear kinematic hardening

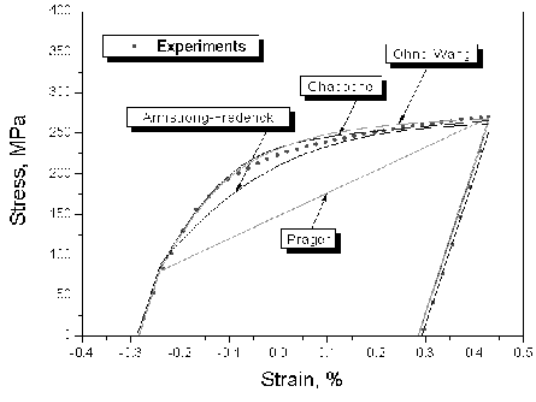

Fig. 5. Comparison of the strain-controlled hysteresis loop between the tests and simulations by each model.

rules, describes the nonlinear behavior well when compared with that of the test throughout the loop locus.

3.3 Stress-controlled cyclic behavior

To investigate the stress-controlled cyclic behavior at a stabilized cycle which has a negligible isotropic softening effect, the stress cycle with the amplitude, 200 MPa and the mean stress, 50 MPa, which can invoke an uniaxial ratcheting behavior, is used in the simulations. Figure 6 shows the simulation results of the stress-controlled cyclic behavior for a stabilized cycle. As expected in the strain-controlled results, the hysteresis loop by the Armstrong-Frederick model provides a relatively large strain increment when compared with that of the Chaboche model and the Ohno-Wang models. Therefore, it is presumed that the Armstrong-Frederick model, which uses only a single backstress equation with the parameters of C and γ, might result in a considerable overestimated inelastic strain with an increasing number of the cycles. This indicates the deficiency of the Armstrong-Frederick model for a ratcheting simulation. When comparing the overall stress-controlled cyclic behavior by the Chaboche mode with the Ohno-Wang model, both reveal a similar behavior but the former presents slightly larger strain values than the latter.

3.4 Ratcheting behavior

To investigate the ratcheting behavior by each constitutive model, the stress-controlled cycles with the stress amplitude, 310 MPa and the mean stress, 70 MPa are applied to each model. Figure 7 shows the simulation results of the cyclic behavior obtained by each model. As shown in Fig. 7(a), the Armstrong-Frederick model provides a relatively large accumulation of the ratcheting strain when compared with that of the Chaboche model and the Ohno-Wang model. The ratcheting parameters, γ_3 for the Chaboche model and m_i for the Ohno-Wang model, are 80 and 0.4 respectively. As shown in Fig. 7(b), the ratcheting strain reaches a constant rate after about the 10^{th} cycle but after the 40^{th} cycle it gradually increases with the cycles. For the Ohno-Wang model, the steady rate of the ratcheting strain starts quickly after 2 or 3 cycles and it accumulates steadily but after about the 20^{th} cycle, the ratcheting strain significantly increases again just like the progressive strain instability. Figure 8 shows the accumulated ratcheting strain representing the maximum peak strain at each cycle. The ratcheting instability phenomena occurring in the modified 9Cr-1Mo steel is discussed further in the next section.

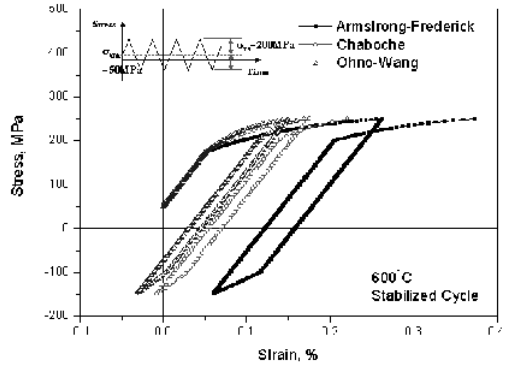

Fig. 6. Comparison of the stress-controlled cyclic behavior for the ratchet loading condition.

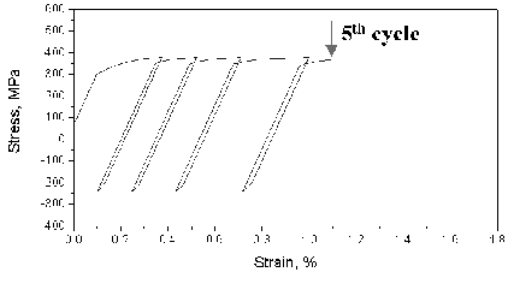

(a) Armstrong-Frederick model

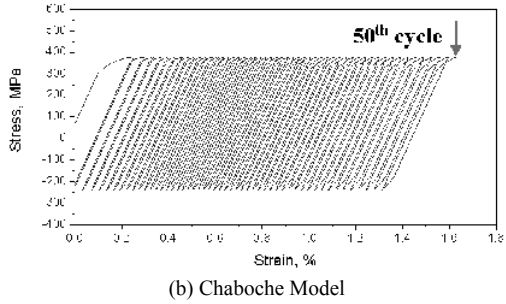

(b) Chaboche Model

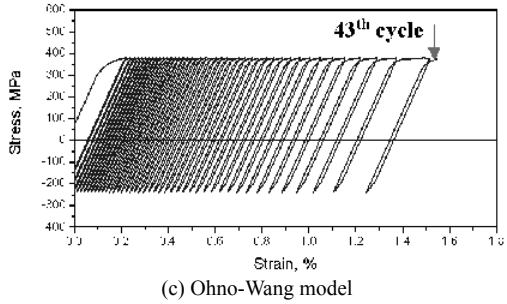

(c) Ohno-Wang model

Fig. 7. Comparison of the Cyclic Ratcheting Behavior.

3.5 Cyclic instability of ratcheting behavior

Actually the ratcheting simulations have to be performed by including the cyclic hardening or softening characteristics. Due to the significant cyclic softening characteristics of the modified 9Cr-1Mo steel as shown in the test results of Fig. 3, the maxi-mum applied load with the constant stress amplitude and the mean stress can become an overload condition after a certain number of cycles. This means that the steady rate of the ratcheting strain can be suddenly changed, and rapidly increase when the applied maximum load reaches a certain level.

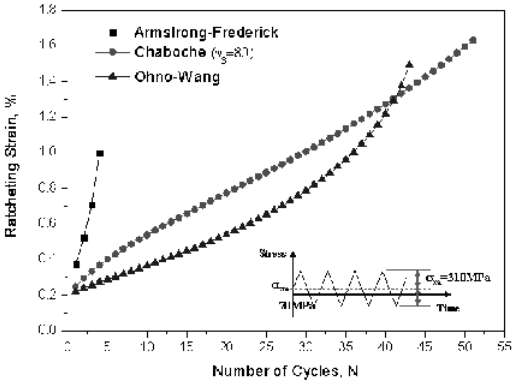

Fig. 8. Number of cycles vs ratcheting strain by the simulations.

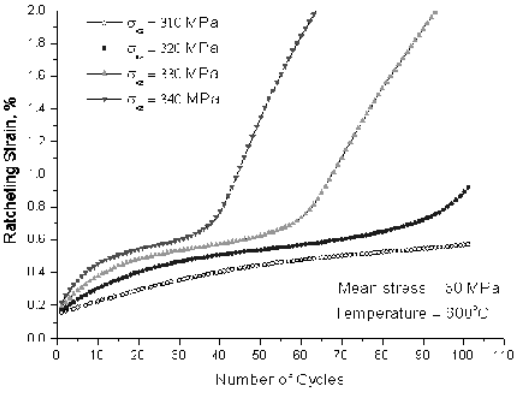

Fig. 9. Effects of the applied stress amplitude on the ratcheting instability of Mod.9Cr-1Mo steel.

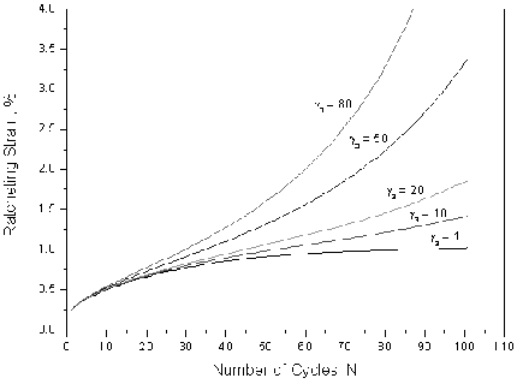

Fig. 10. Effects of the ratcheting parameter, γ_3 on the ratcheting instability of Mod.9Cr-1Mo steel.

Figure 9 shows the effects of the stress amplitudes on the ratcheting strain in the case of the mean stress, 30 MPa. As shown in the results, when the applied stress amplitude is 310 MPa, there is no cyclic instability but by increasing the stress amplitude levels, a progressive cyclic instability occurs after a certain cycle and it starts at a much earlier cycle.

To investigate the effects of the ratcheting parameter, γ_3 in the Chaboche model on the simulation of the cyclic instability, the sensitivity studies were carried out. As shown in the simulation results of Fig. 10, by increasing the value of γ_3 the ratcheting rate becomes large and a severe strain instability occurs with an increase of the number of cycles. Therefore, the γ_3 parameter in the Chaboche model governs the ratcheting strain rate and the stain instability in a cyclic softening material like the modified 9Cr-1Mo steel.

4. Conclusions

In this paper, the inelastic constitutive models for the simulation of the cyclic softening behavior of modified 9Cr-1Mo steel were investigated at an elevated temperature. From the computer simulations by using the inelastic constitutive parameters obtained by using the test data, it is found that the Armstrong-Frederick model was very simple but not adequate enough to simulate a stress-controlled cyclic behavior like a ratcheting due to a significant over-prediction of the ratcheting rate and no controllable parameters for describing a ratcheting instability for a cyclic softening material. However, the Chaboche and the Ohno-Wang models, which overcome a deficiency of the Armstrong-Frederick model, can describe ratcheting phenomena including a cyclic instability very well.

From the simulation results by using the Chaboche model, it was found that the modified 9Cr-1Mo steel might be cyclically unstable due to its cyclic softening characteristics when subjected to a certain level of a severe ratchet loading condition.

Acknowledgment

This project has been carried out under the Nuclear R & D Program by MOST.

Nomenclature

a_{ij}	:	Total backstress tensor
$\dot{a}_{ij}$	:	Incremental total backstress tensor
a_k	:	k component of total backstress
D_{ijkl}	:	Elasto-plastic modulus tensor
E	:	Young's modulus
E_{ijkl}	:	Forth-order elastic modulus tensor
F	:	Loading function
dF	:	Loading increment
f	:	Yield function
$\dot{f}$	:	Evolution of yield function
g	:	Plastic potential function
H	:	Generalized plastic modulus
m	:	Total number of decomposed kinematic hardening rules
m_i	:	Multiplier
$\dot{p}$	:	Magnitude of plastic strain tensor (=$\mid \dot{\varepsilon}^p \mid$)
R	:	Drag stress
α_{ij}	:	Deviatoric backstress tensor
$\dot{\alpha}_{ij}$	:	Incremental deviatoric backstress tensor
ε_{ij}	:	Strain tensor
$\dot{\varepsilon}^e_{ij}$	:	Elastic strain increment tensor
$\dot{\varepsilon}^p_{ij}$	:	Plastic strain increment tensor
ε^{in}	:	Inelastic strain tensor
ε^p_L	:	Plastic axial strain amplitude of a strain-controlled hysteresis loop
σ	:	Stress tensor
σ_{ij}	:	Cauchy stress tensor
$\dot{\sigma}_{ij}$	:	Stress increment tensor
σ_{xa}	:	Amplitude of axial stress cycle
σ_{xm}	:	Mean of axial stress cycle
σ_{yo}	:	Initial yield stress
λ	:	Positive scale factor
τ_{ij}	:	Deviatoric stress tensor
ν	:	Poisson's ratio

References

Armstrong, P. J. and Frederick, C. O., 1966, "A Mathematical Representation of the Multiaxial Bauschinger Effect," *CEGB Report RD/B/N731*, Berkeley Nuclear laboratories.

Bari, S. and Hassan, T., 2000, "Anatomy of Coupled Constitutive Models for Ratcheting Si-mulation," *Int. J. Plasticity*, Vol. 16, pp. 381~409.

Chaboche, J. L. and Rousselier, G., 1983, "On the Plastic and Viscoplastic Constitutive Equations – Part I: Rules Developed with Internal Variable Concept," *Journal of Pressure Vessel Technology*, Vol. 105, pp. 153~158.

Chaboche, J. L. and Rousselier, G., 1983, "On the Plastic and Viscoplastic Constitutive Equations – Part II: Application of Internal Variable Concepts to the 316 Stainless Steel," *Journal of Pressure Vessel Technology*, Vol. 105, pp. 159~164.

Chaboche, J. L., 1989, "Constitutive Equations for Cyclic Plasticity and Cyclic Viscoplasticity," *Int. J. Plasticity*, Vol. 5 pp. 247~302.

Chaboche, J. L., 1991, "On Some Modifications of Kinematic Hardening to Improve the Description of Ratcheting Effects," *Int. J. of Plasticity*, Vol. 7, pp. 661~678.

Han, D. H, et al., 2004, KALIMER-600 Preli-minary Conceptual Design Report, KAERI/TR-2784/ 2004, KAERI.

Nibe, N., Simakawa, Y., et.al, 2001, "Feasibility Studies on Commercialzed Fast Breeder Reactor System (1)–Sodium Cooled Fast Breeder Reactor," Transactions of SMiRT-16,2001.

Ohno, N. and Wang, J. D., 1993, "Kinematic Hardening Rules with Critical State of Dynamic Recovery, Part I: Formulations and Basic Features for Ratcheting Behavior," *Int. J. of Plasticity*, Vol. 9 pp. 375~390.

Prager, W., 1956, "A New Method of Analyzing Stresses and Strains in Work Hardening Plastic Solids," *J. of Applied Mechanics*, Vol. 23, pp. 493~496.

Ruggles, M. B., Ogata, T., 2004, "Creep-Fatigue Criteria and Inelastic Behavior of Modified 9Cr01Mo Steel at Elevated Temperatures," *Oak Ridge National Laboratory*, ORNL/M-3198.

Simo, J. C. and Talyor R. L., 1985, "Consistent Tangent Operator for a Rate-Independent Elasto-plasticity," *Computer Method in Applied Mechanics and Engineering*, Vol. 48, pp. 101~118.

Yaguchi, M. and Takahashi, Y., 2005, "Ratcheting of Viscoplastic Material with Cyclic Softening, Part 1: Experiments on Modified 9Cr-1Mo Steel," *Int. J. Plasticity*, Vol. 21, pp. 43~65.

Yaguchi, M. and Takahashi, Y., 2005, "Ratcheting of Viscoplastic Material with Cyclic Softening, Part 2: Application of Constitutive Models," *Int. J. Plasticity*, Vol. 21, pp. 835~860.